

Piezoresistance of Indium Antimonide*

ROY F. POTTER†

National Bureau of Standards, Washington, D. C.

(Received July 12, 1957)

By applying a tensile stress to specially prepared and oriented samples, the piezoresistivity coefficients of both *n*- and *p*-type indium antimonide have been measured over the temperature range 77°K to 300°K. The results for extrinsic *p*-type material are similar to those for *p*-type Si and Ge, indicating that the valence band structure is similar. Extrinsic *n*-type InSb results confirm the picture of a conduction band having its minimum at the center of the Brillouin zone. The largest effect that was observed in intrinsic material was in the volume coefficient and can be attributed to the change in the forbidden gap due to dilatation of the lattice. The value of this change of gap per unit strain was estimated to be $E_{ig} = -7.0$ ev.

I. INTRODUCTION

OF all the compounds with the zincblende lattice, indium antimonide has undergone the most intensive and extensive study of its electronic transport properties. These studies have been made in the period from 1952 until the present¹ and, indeed, are continuing. The zincblende or sphalerite-type lattice consists of two interpenetrating face-centered-cubic sublattices similar to the diamond lattice except that each sublattice is made up with its respective atom. The symmetry point group is designated T_D and has cubic symmetry.

The present experiment was undertaken in the hope that current ideas about the energy band structure for InSb would have further experimental confirmation or that new concepts would result. The band structures for Ge and Si² described theoretically by Herman have been established recently, largely by application of the "simple many-valley" transport-properties theory to several experiments.³ One of the main features of the structures is that the conduction band minimum does not occur at $k = (0,0,0)$ in wave-vector space for either Ge or Si. On the other hand InSb has been considered to have a conduction band minimum at the center of the Brillouin zone⁴ and the results on *n*-type material described below bear this out.

The valence band structures for Ge and Si are considered to consist of two bands degenerate at the center of the zone. However, one band has a much smaller effective mass than the other. Both bands are warped, but possess cubic symmetry. The results of the present

measurements on *p*-type InSb do not show any qualitative differences from the piezoresistivity of *p*-type Si and Ge. The piezoresistive effect is the specific change of resistivity with applied stress X_j .

$$\Delta\rho_i/\rho_0 = \sum_j \pi_{ij} X_j = \sum_j m_{ij} \mu_j, \quad (1)$$

where the piezoresistance coefficients, π_{ij} , and the elastoresistance coefficients, m_{ij} , are the elements of fourth-rank tensors analogous to the elastic constants, and μ_j is the strain associated with the applied stress.

For cubic crystals with the most common symmetries one has three independent coefficients, π_{11} , π_{12} , and π_{44} (or m_{11} , m_{12} , and m_{44}), referred to the cubic axes. As discussed by Smith,⁵ who first reported the large coefficients observed for Ge and Si, three independent measurements are needed if one is to determine the tensor elements completely.

The longitudinal measurement is made with the current parallel to the applied stress:

$$\Delta\rho/(\rho_0 X) = \pi_{11}' = \pi_{11} - 2\Gamma\pi', \quad (2)$$

where $\pi' = \pi_{11} - \pi_{12} - \pi_{44}$, and the orientation function Γ is given by $l_1^2 m_1^2 + l_1^2 n_1^2 + m_1^2 n_1^2$, l_1 , m_1 , and n_1 being the direction cosines of the specimen axis along which the stress is applied.

The transverse measurement is made with the current and applied stress normal to each other. In this case, the specific change in resistivity with stress is given by

$$\Delta\rho/(\rho_0 X) = \pi_{12}' = \pi_{12} + \gamma\pi', \quad (3)$$

and

$$\gamma = l_1^2 l_2^2 + m_1^2 m_2^2 + n_1^2 n_2^2,$$

where l_j , m_j , and n_j are the direction cosines for the current direction in one set and the applied stress direction in the other.

For isotropic compression one deduces the relationship $-\Delta\rho/(\rho_0 X) = \pi_{11} + 2\pi_{12}$; measurements of this type on InSb have been reported by Keyes⁶ and Long.⁷

Smith⁵ discussed the conversion of the π elements to

* This research was supported by the United States Air Force through the Air Force Office of Scientific Research of the Air Research and Development Command.

† Present address: U. S. Naval Ordnance Laboratory, Corona, California.

¹ A partial list of references includes H. Weiss, Z. Naturforsch. **8A**, 463 (1953); Harman, Willardson, and Beer, Phys. Rev. **95**, 699 (1954); Breckenridge, Blunt, Hosler, Frederikse, Becker, and Oshinsky, Phys. Rev. **96**, 571 (1954); H. P. R. Frederikse and E. V. Mielczarek, Phys. Rev. **99**, 1889 (1955); H. P. R. Frederikse and R. F. Blunt, Proc. Inst. Radio Engrs. **43**, 1828 (1955); Hrostowski, Morin, Geballe, and Wheatley, Phys. Rev. **100**, 1672 (1955).

² F. Herman, Phys. Rev. **93**, 1214 (1954).

³ C. Herring, Bell System Tech. J. **34**, 237 (1955).

⁴ F. Herman, J. Electronics **1**, 103 (1955).

⁵ C. S. Smith, Phys. Rev. **94**, 42 (1954).

⁶ R. W. Keyes, Phys. Rev. **99**, 490 (1955).

⁷ D. Long, Phys. Rev. **99**, 388 (1955).

the m elements and shows for cubic crystals that

$$m_{44} = \pi_{44} C_{44},$$

$$(m_{11} - m_{12})/2 = (\pi_{11} - \pi_{12})(C_{11} - C_{12})/2, \quad (4)$$

$$(m_{11} + 2m_{12})/3 = (\pi_{11} + 2\pi_{12})(C_{11} + 2C_{12})/3,$$

where the C_{ij} are the elastic constants.

II. EXPERIMENTAL

The procedure used in these experiments is similar to that reported by Smith⁵ in that a tensile stress is applied along the length of a sample while the current is either parallel or normal to the sample axis. As a more detailed description of the apparatus is being reported elsewhere,⁸ only the main features will be outlined here.

The samples used were cut from InSb plates that were ground to the desired thickness by standard lapping techniques. An ultrasonic cutting tool was used to cut the sample with four side arms and two dumbbell-shaped ends with a hole through each end. Each end of the sample could be placed in a clevis with a pin. The lower clevis was held to the frame by a ball and socket arrangement while the upper was attached to piano wire which transmitted the tensile stress. With this arrangement, the stress could be applied along the sample axis with no further adjustments necessary. Suitable electrodes were applied in a conventional manner, using indium as a solder. The four-probe method was used for longitudinal measurements while a two probe method had to be used for the transverse. In this case, the sides between the side arms were plated with copper and the potential and current leads soldered onto the arms.

The tensile stress was applied by means of a balance beam where increments of 100 grams of load could be applied up to 1000 grams. The fulcrum could be adjusted in position to compensate for changes due to plastic strain or thermal expansion of the load-bearing piano wire. The balance beam, load-bearing wire, and sample were in the same enclosure which could be evacuated or filled with helium gas of a suitable pressure. The glass and brass chamber containing the balance beam and fulcrum was connected to the sample can by a stainless steel tube. Coaxial to this tube was another stainless steel tube through which the piano wire was placed to keep it from fouling the electrical leads. The sample can was equipped with a heater for temperature control.

The results reported here are for temperatures between 77°K and 300°K. For this range, a Pyrex envelope was placed about the can and stainless steel tube while liquid nitrogen in turn was placed about the envelope. An atmosphere of He gas (room temperature) was admitted to the sample can, and by adjusting the current through the heater and the pressure in the

TABLE I. Hall coefficient and conductivity data for InSb samples F , H , L , J , O , and P at 77°K.

Sample	R_H cm ³ /coul	σ (ohm ⁻¹ cm ⁻¹)	σR_H cm ² /V-sec	$p-n$ cm ⁻³	Orientation of axis
F	+6110	0.69	4220	1.02×10^{15}	(210)
H	+7180	0.61	3660	0.87×10^{15}	(100)
L	+1360	4.46	6070	4.60×10^{15}	(100)
O	-1970	109	215 000	-3.18×10^{15}	(210)
P	-1680	78.1	131 000	-3.73×10^{15}	(100)
J	-8360	41.7	348 000	-0.74×10^{15}	(100)

Pyrex envelope, an intermediate range of temperatures was available for the measurements.

The samples were oriented by x-ray back-reflection photo technique. The crystals as pulled had their axes very nearly oriented along the (001) direction and slices normal to this direction were cut and ground by standard lapping procedures until the slices had parallel sides and were 1.0–1.2 mm thick. These slices were re-examined by x-rays and either the (100) or (210) directions determined. Samples with their axes along their axes along the desired directions were then cut on the ultrasonic cutting device. The principal error in the orientation procedure lies in the (001) determination but was still less than 1°.

The electrical measurement technique was quite conventional, a Leeds and Northrup type- K potentiometer being used. A breaker-type dc amplifier with 10⁴-ohm input impedance was used in place of a galvanometer. The output of the amplifier was fed into a strip recorder. Before the measurements the potentiometer was balanced; an increment of load was then applied to the sample and the deflection of the recorder noted. For large deflections, the signal change was checked by rebalancing the potentiometer. Although the precision and accuracy were quite good for p -type samples at 77°K where the resistance and the effect were relatively large, at higher temperatures the resistance decreased markedly as the samples became intrinsic and the accuracy obtained was lessened. The same considerations hold for n -type samples except the situation was worse as far as precision at 77°K was concerned because the effect is also relatively small. The precision varied from 1% for the longitudinal measurements at 77°K to 10% for the others at room temperature.

Another source of error in the transverse case was discussed by Smith.⁵ The current lines are not normal to the axes at the ends of the electrodes, and when an anisotropic resistivity tensor results because of the strain, the transverse measurements must be corrected. By having the copper plating extend along one edge of each sidearm, the need for this correction is minimized as the region in which the field lines are distorted is highly localized. Nevertheless, as no corrections for this transverse measurement were made, there does exist the possibility of errors in the transverse measurements.

The quantities that were measured in this experiment give the relative change of resistance with applied

⁸ R. F. Potter and W. J. McKean, J. Research Natl. Bur. Standards 59 (1957).

TABLE II. The values of π_{ij} at 77°K and the principal elastoresistance coefficients obtained from them and the elastic constants based on data from reference 9.

Sample	(10^{-11} cm ² /dyne)	(10^{-11} cm ² /dyne)	(10^{-11} cm ² /dyne)	$\frac{1}{3}(m_{11}+2m_{12})$	$\frac{1}{3}(m_{11}-m_{12})$	m_{44}
<i>F, H</i>	+8.6	-4.2	+32.3	-4.4	+21.0	+101
<i>L</i>	+10.4	-4.5	...	+6.2	+24.6	...
<i>O, P</i>	-1.70	-1.0	-0.4	-16.0	-1.1	-1.3
<i>J</i>	-1.69

($C_{11}+2C_{12}$)/3 = 4.45×10^{11} dynes/cm²; ($C_{11}-C_{12}$)/2 = 1.65×10^{11} dynes/cm²; C_{44} = 3.14×10^{11} dynes/cm².

stress. As discussed in references 5 and 8, these quantities were converted to give the relative changes in resistivity by adding or subtracting the appropriate elastic constants.

III. RESULTS

Measurements have been made on 6 samples of InSb, 3 *p*-type and 3 *n*-type specimens. Table I lists the conductivity and Hall coefficient data taken at 77°K. From these data, the Hall mobility and impurity concentration have been calculated and are also shown in Table I.

A. *p*-Type Samples

Samples *F* and *H* were cut from adjacent slabs of the crystal; they have similar electrical characteristics and are considered as a pair.

Table II contains π_{ij} values determined at 77°K. From these figures and the elastic constants of InSb⁹ the elastoresistance coefficients have been evaluated. At this temperature all samples measured were in the exhaustion region; hence we are looking at the properties of extrinsic material. It is worthy to note that the results of extrinsic *p*-type InSb are very similar to those for *p*-type extrinsic Si and Ge⁵ in that

$$m_{44} > (m_{11} - m_{12})/2 \gg (m_{11} + 2m_{12})/3.$$

The values of m_{44} for all three materials are of the same order of magnitude and of the same sign. The coefficient $(m_{11} - m_{12})/2$ for InSb is relatively larger while the volume coefficient $(m_{11} + 2m_{12})/3$ is quite small. Similar results have been reported by Tuzzolino¹⁰ except that his value for m_{44} is higher.

Electrons in InSb have such a high mobility and small effective mass that they show their influence on the electrical properties at temperatures considerably below the intrinsic range. This is apparent in Fig. 1 where the temperature variations of π_{11} and π_{12} are shown for sample *L*.

π_{11} changes sign from positive to negative in much the same manner that the Hall coefficient does. Although π_{12} values keep the negative sign, the magnitude increases sharply and goes through a maximum as the intrinsic range is reached.

⁹ R. F. Potter, Phys. Rev. **103**, 47 (1956).

¹⁰ A. J. Tuzzolino, Phys. Rev. **105**, 1411 (1957), and private communication.

The very marked effect of temperature on the volume effect is shown in Fig. 2. Also shown, for purposes of comparison, are values that have been scaled from the data published by Keyes⁶ and Long⁷ who measured the resistance as a function of applied hydrostatic pressure. The points shown in Fig. 2 were taken from the slopes of the published curves but restricted to the linear region at very low pressures. The temperatures at which the magnitude maximum occurs, as well as the magnitude itself, are both extremely sensitive to the sample purity as can be seen from Fig. 2. Keyes quotes a figure of $10^{17}/\text{cc}$ for his samples which is to be compared with less than $10^{15}/\text{cc}$ for sample *H*. The temperature differences between the respective maxima are 300°C. Tuzzolino,¹⁰ also, has seen a similar variation of π_{11}' with temperature indicating the purity effect.

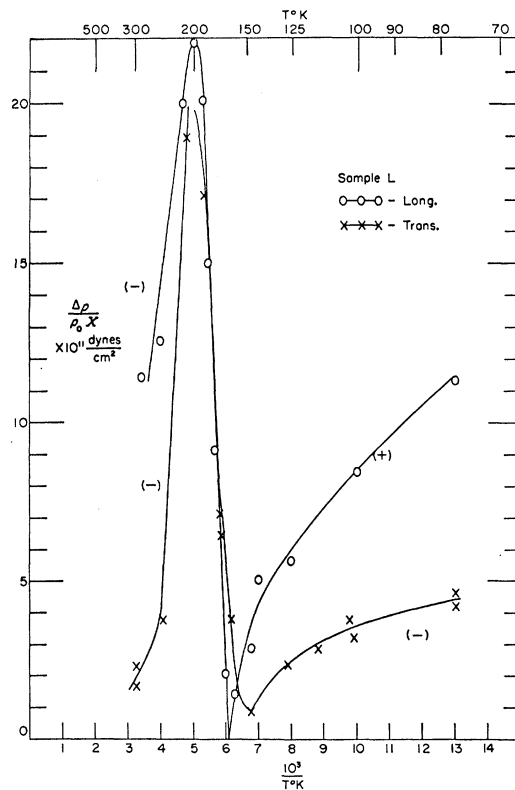


Fig. 1. The piezoresistive effect observed for *p*-type sample *L*. The longitudinal effect suffers a change in sign over the observed temperature range while the transverse remains negative.

B. *n*-Type Samples

The results for the pair of samples *O* and *P* are shown in Fig. 3. In the extrinsic region all the piezoresistance coefficients are very small in magnitude (see Table II) and remain fairly constant as the temperature rises, until the transition region is reached. Sample *J* had a similar behavior for the longitudinal effect except that a maximum in magnitude occurred at 250°K. In contrast to the *p*-type samples, all the coefficients for *n*-type samples have the same sign (negative).

C. Shear Elastoresistance Coefficients

The shear piezoresistance coefficients have been converted to the elastoresistance coefficients m_{44} and $(m_{11}-m_{12})/2$ and are shown in Fig. 4 for all samples. Both coefficients are relatively small in the case of *n*-type material at all temperatures. The fact that the m_{44} of *n*-type material undergoes a change of sign and apparently has a slight positive maximum in the intrinsic region is probably due to the residue effect that holes have on this coefficient. Both *n*- and *p*-type samples show a slight minimum at about 250°K for $(m_{11}-m_{12})/2$. These coefficients are small in magnitude for all samples in the intrinsic range.

IV. DISCUSSION

A. Extrinsic *p* Type

The character of the valence band structure of InSb in particular and zinc blende lattices in general has been

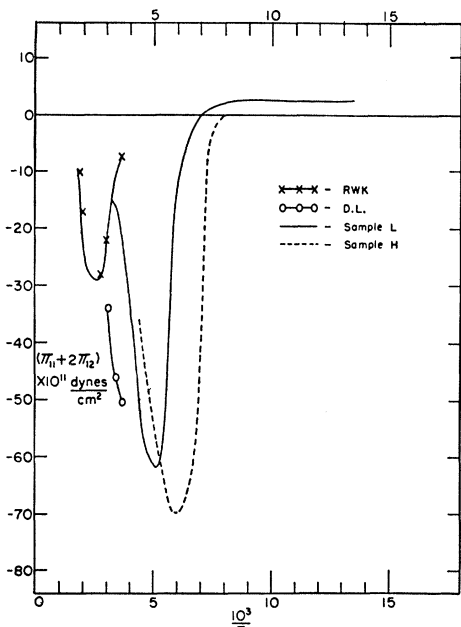


FIG. 2. The volume piezoresistive effect for *p*-type InSb. As the transverse measurements on sample *H* were incomplete, the values shown are based on $3\pi_{11}$. The effect that purity has on the maxima is clearly demonstrated. Curves designated by RWK and DL are data from references 6 and 7, respectively. Keyes' sample had an excess acceptor concentration of $10^{17}/\text{cc}$ while Long's sample was listed as having $3 \times 10^{16}/\text{cc}$.

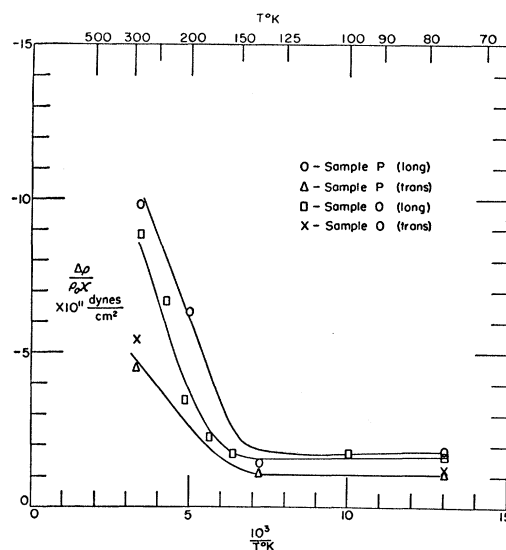


FIG. 3. The piezoresistive effect in *n*-type InSb samples *O* and *P*. The effect is very small in the extrinsic region but increases sharply as the samples become intrinsic.

the subject of recent theoretical studies. Kane¹¹ has applied the $\mathbf{k} \cdot \mathbf{p}$ method to InSb and has presented a picture where there are large-mass bands for holes with maxima on the (111) axes, very close to $\mathbf{k} = (0,0,0)$; a small-mass band is degenerate with these at the center of the Brillouin zone.

Experimental evidence which can supply information concerning critical points in the band structure is lacking. Optical absorption measurements showed a long-wavelength tail which appeared to be due to indirect transitions (nonvertical).¹² Analyses similar to that given by McFarlane and Roberts¹³ for Si and Ge were applied to the data. This was a scheme whereby nonvertical transitions were allowed by means of photon-phonon processes. When the analysis¹² was made for the optical measurements on InSb using only acoustical phonons, the resulting position of the valence band maximum was at a large value of k . Another analysis¹⁴ on the same data pointed out that it was possible that in InSb optical-mode phonons could also play a role in such processes. The resulting value for k_m of the valence band maximum was much smaller, although considerably larger than that for Kane's picture. The use of optical- and acoustical-mode phonons gives results more in line with those of Kane. Another model has been proposed by Dumke,¹⁵ assuming parabolic valence bands with their maxima at the center of the zone and indirect transitions assisted by

¹¹ E. O. Kane, J. Phys. Chem. Solids **1**, 249 (1957).

¹² V. Roberts and J. E. Quarrington, J. Electronics **1**, 152 (1955); Blount, Callaway, Cohen, Dumke, and Philips, Phys. Rev. **101**, 563 (1956).

¹³ G. C. McFarlane and V. Roberts, Phys. Rev. **97**, 1714 (1955); Phys. Rev. **98**, 1865 (1955).

¹⁴ R. F. Potter, Phys. Rev. **103**, 861 (1956).

¹⁵ W. P. Dumke, Bull. Am. Phys. Soc. Ser. II, **2**, 185 (1957).

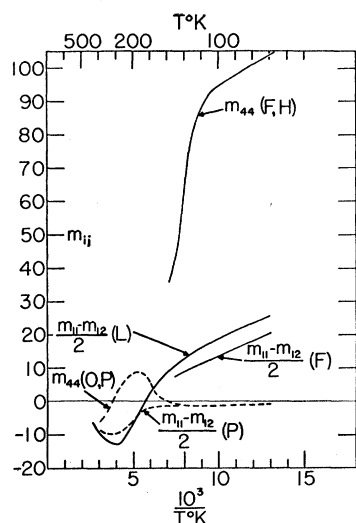


FIG. 4. The shear elastoresistivity coefficients for both n - and p -type InSb. Samples F , H , and L were p -type, while samples O and P were n -type. The constant m_{44} for p -type is the largest constant observed in the extrinsic region and is similar to p -type Ge in this respect. The increase in m_{44} for n -type is likely due to residual effect of strain upon the holes. The quantity $(m_{11}-m_{12})/2$ has a slight minimum for intrinsic n - and p -type material.

optical-mode phonons only. Thus, it appears that these analyses of the indirect transitions, at present, do not give an unqualified affirmation or denial of the fine details of the valence band structure although they do lend support to a picture similar to that of Si and Ge with possible modification as indicated by Kane.

Ge and Si have been pictured as having two valence bands degenerate at $k=(0,0,0)$, each having different effective masses and being warped in k -space. Adams¹⁶ discussed in some detail the elastoresistance coefficients of p -type Si and Ge on the assumption of such a band structure. Although he does not give quantitative answers, he shows that $m_{11}+2m_{12}=0$ because no symmetry change is brought about by uniform dilatation and concludes that m_{44} and $(m_{11}-m_{12})/2$ do not necessarily vanish, i.e., shears can change the warped energy surfaces such as to modify the mobilities. Smith found that m_{44} was quite large for both Si and Ge while $(m_{11}-m_{12})/2$ was considerably smaller. p -type InSb is quite similar to Si and Ge in that m_{44} is large and has approximately five times the magnitude of $(m_{11}-m_{12})/2$. The coefficient m_{44} also has the same sign for all three substances and magnitude of the same order.

It is concluded from these results and from a comparison with the theoretical and experimental results for Si and Ge that the valence band of InSb is not greatly different from that of Ge and Si. Frederikse and Hosler¹⁷ reach a similar conclusion based on their measurements of the magnetoresistance.

B. Extrinsic n Type

That the conduction band of InSb is spherical in shape and located at the center of the reduced zone is borne out by the present measurements. All of the

piezoresistance coefficients have small magnitudes at 77°K (see Fig. 4). The explanation of the small residual effects must wait a refinement of theory and experiment. The absence of gross effects, however, indicates no large anisotropic character of the band. The theoretical discussions⁴ of InSb predict a band that should have this type of behavior under strain. The existence of spherical energy surfaces has been substantiated by other experiments, namely, magnetoresistance measurements¹⁷ and cyclotron resonance.¹⁸

C. Temperature Effects in p -Type InSb

The shear coefficients of extrinsic p -type InSb exhibit behavior similar to that of Si and Ge,¹⁹ namely, they are linear in T^{-1} . Referring to Fig. 4, one notes this apparent linearity between 77°K and 150°K while at temperatures above this the coefficients decrease in magnitude quite sharply as the semiconductor becomes intrinsic. Although the shear coefficients decrease as the intrinsic region is approached, the volume effect $\pi_{11}+2\pi_{12}$ increases in magnitude to a maximum and then decreases in a manner faster than T^{-1} (see Fig. 2). This effect, which is also present for n -type material, is apparently caused by the effect of dilatation of the lattice upon the forbidden band gap. The change in the width of the energy gap in turn affects the number of carriers that can be excited into the conduction band. If the change of gap energy per unit dilatation is positive, the number decreases, and vice versa.

Assuming classical statistics, the following relations hold for semiconductors:

$$\begin{aligned}\sigma &= e(n\mu_n + p\mu_p), \\ n p &= 4(2\pi kT/h^2)^3 (m_n m_p)^3 \exp(-E_g/kT), \\ p - n &= N_A - N_D,\end{aligned}\quad (5)$$

where σ is the conductivity, e the electronic charge, n and p are the concentrations of negative and positive carriers, respectively, μ_n and μ_p their respective mobilities, m_n and m_p their respective effective masses, and $N_A - N_D$ is the excess concentration of acceptors over donors as determined by Hall-effect measurements at 77°K. From Eq. (5) one finds then:

$$\begin{aligned}\frac{(m_{11}+2m_{12})}{3} \frac{\delta \ln \rho}{\delta \ln V} &= \frac{E_{1g}}{2kT} \left(\frac{a-1}{a} \right) \left(\frac{1 + (\mu_p/\mu_n)}{(a-1)/(a+1) + (\mu_p/\mu_n)} \right),\end{aligned}\quad (6)$$

where $a = [1 + 4np/(N_A - N_D)^2]^{1/2}$, and $E_{1g} = \delta E_g / \delta \ln V$ is the gap change per unit dilatation.

In this derivation, the values of μ_n and μ_p were considered to be unaltered by the strain. At low tempera-

¹⁶ E. N. Adams, Chicago Midway Laboratories Report CML-TN-P8, 1954 (unpublished).

¹⁷ H. P. R. Frederikse and W. R. Hosler, Phys. Rev. (to be published).

¹⁸ Dresselhaus, Kip, Kittel, and Wagoner, Phys. Rev. **98**, 556 (1955).

¹⁹ Morin, Geballe, and Herring, Phys. Rev. **105**, 525 (1957).

tures where $a \rightarrow 1$,

$$\delta \ln \rho / \delta \ln V \rightarrow (E_{1g}/kT) [n\bar{p}/(p-n)^2] (\mu_n/\mu_p),$$

while at high temperatures where $a \gg 1$, $\delta \ln \rho / \delta \ln V \rightarrow E_{1g}/2kT$. The parameters used with Eq. (6) are listed in Table III and the results for sample *L* are shown in Fig. 5. Good agreement between the experimental and theoretical maxima is obtained for $E_{1g} = -7.0$ ev.

The temperature and magnitude of the volume-effect extrema are highly dependent on sample purity. In Fig. 2 values taken from work by Keyes⁶ and Long⁷ are shown for comparison with the present work; the shift with temperature of the maxima for samples of varying purity is quite apparent. This effect of purity on the volume coefficient is understandable on the basis of Eq. (6). The calculated curve and experimental curves noticeably fail to agree at higher temperatures. This might be attributed to the degeneracy of the intrinsic material and the nonapplicability of the relationships of Eq. (5).

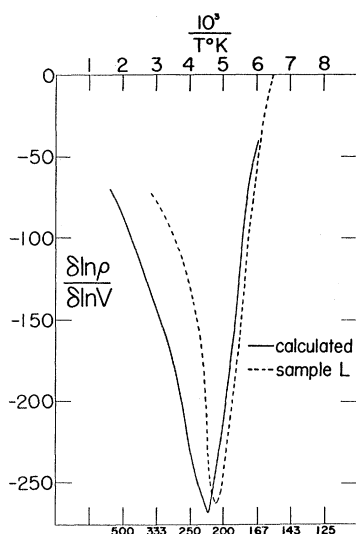


FIG. 5. The volume effect for *p*-type sample *L*. The volume effect is the largest observed for InSb. The calculated curve is based on a value of E_{1g} of -7.0 ev and an acceptor excess of $10^{15}/\text{cc}$.

D. Temperature Effects in *n*-Type InSb

The piezoresistive effect is small for *n*-type over the temperature range 77°K – 100°K , but in the intrinsic range a behavior similar to the *p*-type volume effect is found. However, the shear coefficients are small in magnitude over the entire range as shown in Fig. 4. There is an apparent maximum for m_{44} as the *n*-type samples become intrinsic; this could be due to the residual effect of strain on holes. The other shear constant $(m_{11} - m_{12})/2$ shows a slight minimum at approximately 250°K for both *n*- and *p*-type intrinsic samples. The appearance of this minimum is difficult to understand. Because the electron mobility is so much greater than that of the holes, it is probably not caused by contributions from the valence band. On the other hand, there exists no other evidence in favor of anisotropy of the conduction band.

TABLE III. Parameters used for InSb in connection with Eqs. (6) and (7) of the text.

μ_p/μ_n	m_p/m_e	m_n/m_e	E_g ev	E_{1g} ev	$n\bar{p}e^{0.22/kT}/T^3$ $\text{cm}^{-6} \text{deg}^{-3}$
1/50	0.18	0.013	$0.23 - 2 \times 10^{-4} T$	-7.0	2.95×10^{28}

Turning to the volume effect in *n*-type InSb, one finds a behavior similar to that observed for *p*-type. The results for sample *P* are shown in Fig. 6 along with the data taken from reference 6. Sample *J* had a maximum in π_{11} at about 275°K .

Applying the same analysis for *n*-type samples, one finds:

$$\frac{m_{11} + 2m_{12}}{3} = \frac{\delta \ln \rho}{\delta \ln V} = \frac{E_{1g}}{2kT} \left(\frac{a-1}{a} \right) \times \left(\frac{1 + (\mu_p/\mu_n)}{1 + [(a-1)/(a+1)](\mu_p/\mu_n)} \right) \sim \frac{E_{1g}}{2kT} \left(\frac{a-1}{a} \right), \quad (7)$$

which is somewhat different from Eq. (6), especially at low temperatures where $a \rightarrow 1$ and $\delta \ln \rho / \delta \ln V \rightarrow (E_{1g}/kT) \times [n\bar{p}/(n-p)^2]$. The calculated curves of Fig. 6 are for different values of $N_D - N_A$ but $E_{1g} = -7.0$ ev. The high-temperature agreement with Keyes' data for *n*-type is improved over that for sample *L*, but again the magnitude of the coefficient falls off faster than $E_{1g}/2kT$. This failure is also most likely due to the increasing amount of degeneracy of the samples.

V. SUMMARY

The results of these studies of piezoresistivity in InSb have brought out the following features of the band picture. First, the conduction band minimum is located at the center of the zone and at low-energy values the constant energy surfaces are spherical. This is borne out by the low values of the elastoresistivity of extrinsic

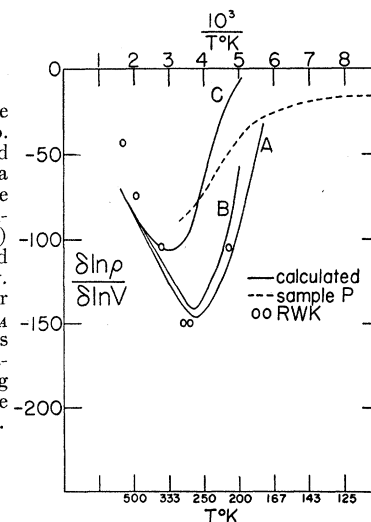


FIG. 6. The volume effect for *n*-type InSb. The points designated RWK are based on data from reference 6, while curves *A* and *B* were calculated from Eq. (7) using $N_D - N_A = 10^{15}$ and 0.7×10^{15} , respectively. Keyes gives a value for his sample of $N_D - N_A = 10^{15}/\text{cc}$. Curve *C* was calculated using the parameters corresponding to sample *P* where $N_D - N_A = 3.7 \times 10^{15}/\text{cc}$.

n-type InSb. Secondly, the valence band maxima are probably very similar to that for Ge and Si; at least, any model which will describe the elastoresistivity of extrinsic *p*-type Ge and Si could undoubtedly be applied to *p*-type InSb. In addition, it does not seem unreasonable that the valence band picture described by Kane would also result in shear-type elastoresistance coefficients like those observed.

The large variation observed for the volume effect $\delta \ln \rho / \delta \ln V$ indicates the effect of lattice dilatation on the forbidden energy gap. By considering that the product np changes with strain only as E_g varies, the deformation potential E_{1g} was determined to be very

nearly -7.0 eV which corresponds to the value determined by Ehrenreich²⁰ from the pressure dependence of the Hall constant given by Long.⁷

VI. ACKNOWLEDGMENTS

It is a pleasure to acknowledge the able assistance in instrumentation given by W. J. McKean. D. E. Roberts provided the single crystals of InSb from which the samples were prepared and W. R. Hosler measured the Hall and conductivity data of Table I. I wish to thank A. J. Tuzzolino for transmitting to me some of his results before publication.

²⁰ H. Ehrenreich, *J. Phys. Chem. Solids* **2**, 131 (1957).

Soft X-Ray Absorption by Thin Films of Vanadium*

BIPIN K. AGARWAL† AND M. PARKER GIVENS

Institute of Optics, University of Rochester, Rochester, New York

(Received July 11, 1957)

The absorption of soft x-rays by vanadium has been measured in the spectral region between 190 Å and 250 Å. The observed absorption band is interpreted as a combination of M_3 and M_2 bands in the ratio of 2:1 and separated by 1.5 eV. The results are compared with previous determinations on chromium and iron.

THE M_{23} absorption bands of vanadium have been measured. This absorption is produced by transitions from the $3P_{3,2}$ states to the unfilled portion of the conduction band. The apparatus and experimental procedure are essentially the same as described previously¹ and will not be discussed here.

Films were prepared by vacuum evaporation onto thin celluloid supports from two parallel tungsten wires 0.050 inch in diameter. The vanadium was vacuum-fused at a pressure of 2×10^{-5} mm Hg. During evaporation the pressure was kept below 10^{-4} mm Hg and the evaporator was kept cool by intermittent evaporation. Currents of approximately 12 amp were used for 15-second intervals, between which the system was allowed to pump down to the original vacuum. In this way films of the required thickness were built up.

The films ranged in thickness from 25 Å to 300 Å. Absorption was determined by comparing the transmission of two films of different thicknesses but which were otherwise identical in preparation. The difference of thickness between the two films used for any one run was kept between 130 Å and 140 Å.

Film thicknesses were determined by measuring the optical density in visible light, the optical density νs

thickness curve having been previously determined by using fringes of equal chromatic order.² The vanadium was obtained from Jarrell-Ash Company containing as chief impurities 0.04% iron, 0.044% carbon, and 0.085% oxygen.

Results of the absorption measurements are shown in Fig. 1. The solid curve represents the average of three independent runs, two runs on one set of samples and one on another set prepared in a separate evapo-

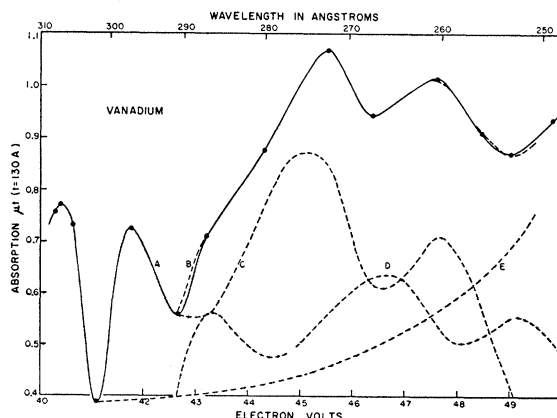


Fig. 1. The soft x-ray absorption band of vanadium and its components. A—experimental curve; B—sum of curves C, D, and E; C and D—suggested M_3 and M_2 bands; E—background.

* This research was supported by the National Science Foundation.

† On leave from the Physics Department, University of Allahabad, Allahabad, India.

¹ M. P. Givens and W. P. Siegmund, *Phys. Rev.* **85**, 313 (1952); also B. K. Agarwal and M. P. Givens, *Phys. Rev.* **107**, 62 (1957).

² S. Tolansky, *Multiple Beam Interferometry* (Oxford University Press, New York, 1948), Chap. 8.